Electronic Supplementary Material (ESI) for Materials Chemistry Frontiers.

Supplementary Information for

Broad-Spectral-Response Perovskite Photodetector with High On/Off Ratio and High Detectivity

Xiaohui Yi[1,2], Yisen Wang[1], Ningli Chen[2]， Zhiwei Huang[1], Zhenwei Ren[2], Hui Li[2], Tao Lin[*2], Cheng Li[*1],and Jizheng Wang[*2,3]

[1] Semiconductor Photonics Research Center, OSED, Department of Physics, Xiamen University, Xiamen, Fujian 361005, China
E-mail: lich@xmu.edu.cn

[2] Institute of Chemistry, Chinese Academy of Sciences, Beijing 100190, China
E-mail: jizheng@iccas.ac.cn

[3] University of Chinese Academy of Sciences, Beijing 100049, China
E-mail: jizheng@iccas.ac.cn

Keywords: $CH_3NH_3PbI_3$, hybrid, photodetector, high on/off ratio, high detectivity

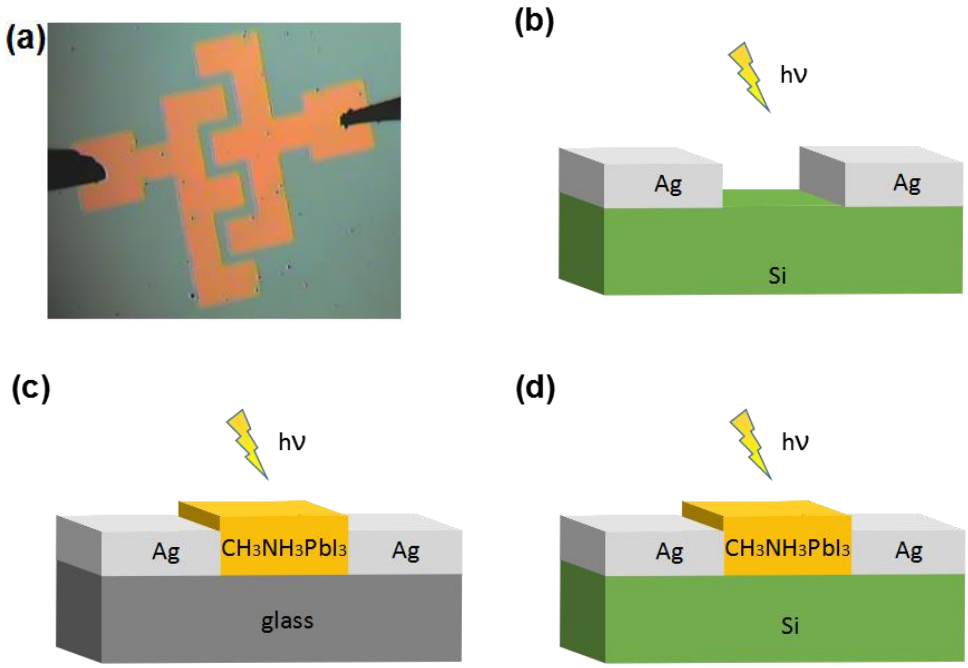

Fig. S1 a) The optical microscopy image of a $CH_3NH_3PbI_3/TiO_2$/Si PD. Schematic structures of b) the Si PD, c) $CH_3NH_3PbI_3$/glass PD, and d) $CH_3NH_3PbI_3$/Si PD.

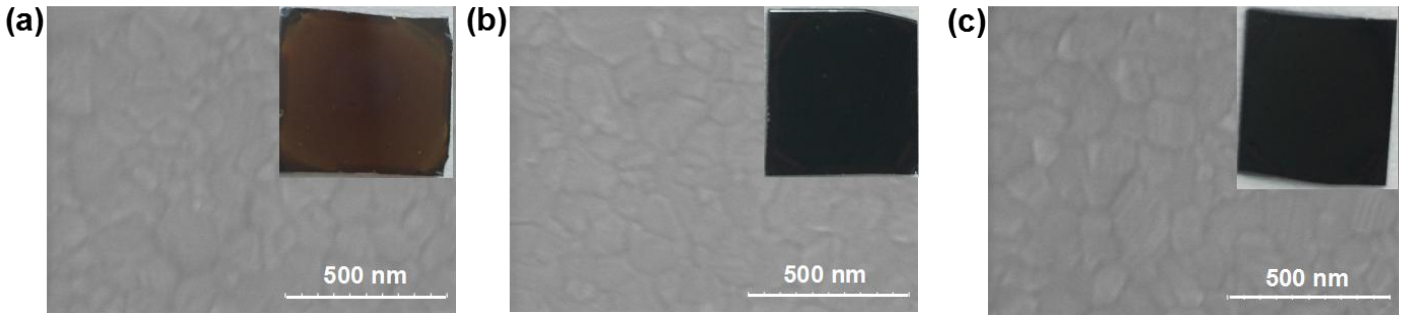

Fig. S2 Top-view SEM images and camera photos (inserted top corner) of a) the $CH_3NH_3PbI_3$/glass, b) $CH_3NH_3PbI_3$/Si, and c) $CH_3NH_3PbI_3/TiO_2$/Si.

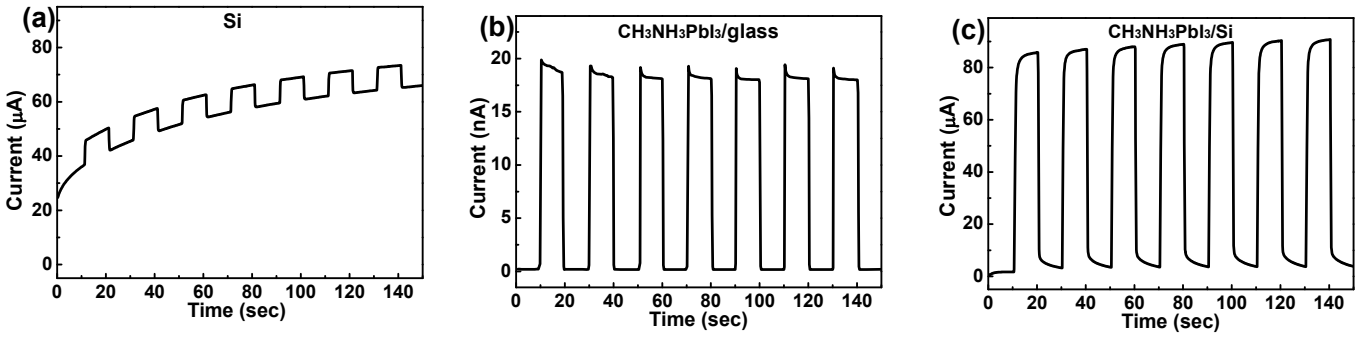

Fig. S3 On-off switching properties of a) the Si PD, b) $CH_3NH_3PbI_3$/glass PD, and c) $CH_3NH_3PbI_3$/Si PD.

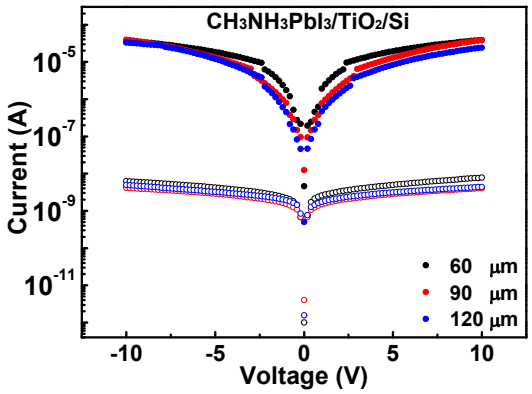

Fig. S4 The dark current and light current the $CH_3NH_3PbI_3/TiO_2$/Si PDs with a channel width of 60, 90 and 120 μm as a function of applied voltage (under white light illumination of 0.5 mW cm^{-2}).

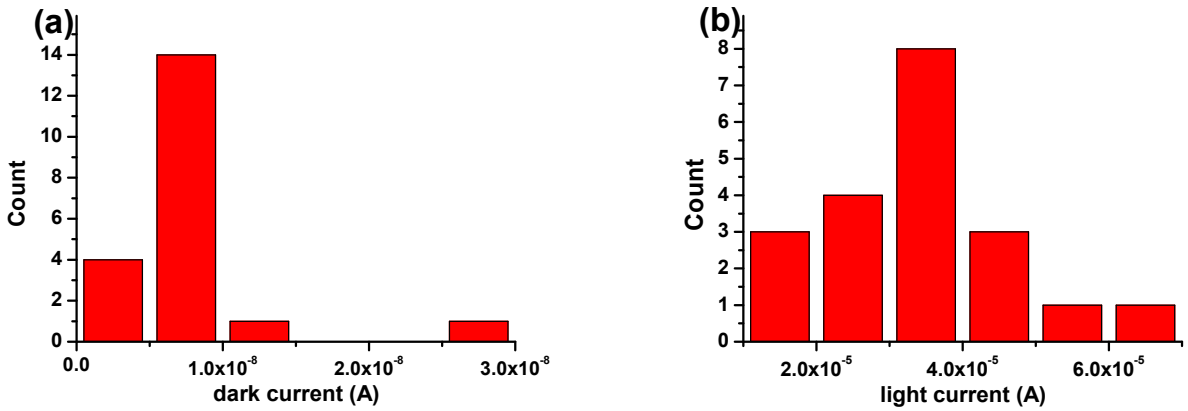

Fig. S5 The histogram of dark current and light current at a bias of 10 V for the $CH_3NH_3PbI_3/TiO_2$/Si PD

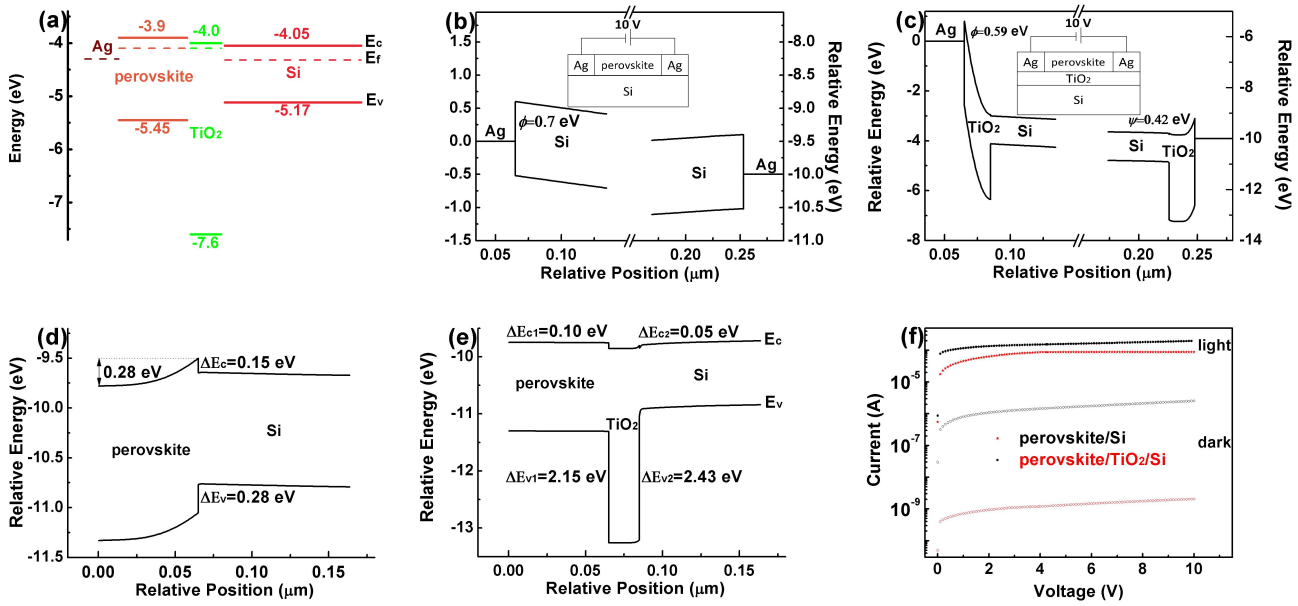

Fig. S6 a) Band diagrams of the materials. Band diagram of the junctions under a bias of 10 V and in dark: b) the Ag/Si junctions in the $CH_3NH_3PbI_3$/Si PD; c) the Ag/TiO_2/Si junctions in the $CH_3NH_3PbI_3$/TiO_2/Si PD; d) the $CH_3NH_3PbI_3$/Si junction; e) $CH_3NH_3PbI_3$/TiO_2/Si junction. f) The simulated dark current and light current of the two PDs. ψ is Schottky barrier, and ϕ is the build-in potential inside the TiO_2 layer.

On/off ratio, responsivity and detectivity

Let's define I_p and I_d as the light current and dark current, respectively. P_{in} is the illumination power density. A is the active area. Δf is the electrical bandwidth and i_{noise} is the noise current. q is the absolute value of electron charge (1.6×10^{-19} C).

On/off ratio (r) is defined as: $r = \frac{I_p}{I_d}$

Responsivity (R) is defined as: $R = \frac{I_p - I_d}{A \cdot P_{in}}$

Detectivity (D^*) is defined as: $D^* = R \cdot \frac{\sqrt{A\Delta f}}{i_{noise}} = R \cdot \frac{\sqrt{A}}{\sqrt{2qI_d}}$ （Assuming the noise current is dominated by the shot noise,[1] hence: $i_{noise} \approx \sqrt{2qI_d\Delta f}$ ）

Device Simulation

To explore the physical nature of the role the TiO_2 layer plays in reducing the dark current, we

performed a general device simulation based on the fundamental drift-diffusion charge transport model via a commercial technology computer aided design platform,[2,3] the material parameters used in the simulation are listed in Table S1. The energy levels of the $CH_3NH_3PbI_3$, TiO_2, Si and Ag (including conduction band edge, valence band edge and Fermi level) are presented in Figure S5a. In the $CH_3NH_3PbI_3$/Si PD, the two Ag electrodes form two Schottky junctions with the $CH_3NH_3PbI_3$ film, which are shown in Figure S5b under a bias of 10 V and in dark condition. The left Ag electrode injects electrons into Si, and the electrons are transported in Si towards to the right electrode, which then collects the electrons. The injection process has to overcome a barrier of 0.7 eV, but the collection process should be quite smooth since there is no obvious potential barrier that blocks the electrons from dropping into the right Ag electrode. In case of the $CH_3NH_3PbI_3$/TiO_2/Si PD shown in Figure S5c, electrons should be injected from the left Ag electrode into the TiO_2 by overcoming a high barrier of 0.59 eV, then flow into Si. In the collection process, the electrons have to overcome a high barrier of 0.42 eV to jump into the right electrode from the TiO_2. Such a high barrier in the collection side significantly reduces the dark current of the PD. Under illumination, in the $CH_3NH_3PbI_3$/Si PD, photoholes in the $CH_3NH_3PbI_3$ film will drop into Si, and photoelectrons will be left in the $CH_3NH_3PbI_3$ film (judged from the band diagram of the $CH_3NH_3PbI_3$/Si junction shown in Figure S5d). Whereas in the $CH_3NH_3PbI_3$/TiO_2/Si PD, photoholes will be blocked by the TiO_2 layer and left in the $CH_3NH_3PbI_3$ film, and photoelectrons will drop into the TiO_2 film and then flow into Si (Figure S5e). In both cases, photogenerated electrons and holes generated in the $CH_3NH_3PbI_3$ film are spatially separated, leading to the observed PL quenching in Figure 3b. Meanwhile, under illumination (especially strong illumination), rich photocarrier would fill into the Ag/Si, and Ag/TiO_2 junction regions, significantly reducing the barrier height, or in other words, the Ag/Si, and Ag/TiO_2 contact resistances. This is the reason that the light current of the $CH_3NH_3PbI_3$/TiO_2/Si PD does not drop much (only a little) in comparison to that of the $CH_3NH_3PbI_3$/Si PD. The carrier mobility in Si is much higher than that in the $CH_3NH_3PbI_3$ film, so the photocurrent is dominantly from carrier transport in Si. Due to the spatial separation of electrons and holes, the carrier lifetime is greatly prolonged, thereby a large gain can be achieved. The simulated dark current and light current of the two PDs are given in Figure S5f, which is characteristically consistent with the experiment observations (Figure 4b): the dark current is greatly reduced while the light current is only slightly decreased when the TiO_2 layer is used.

Table S1. Parameters used in the device simulation.

parameter	$CH_3NH_3PbI_3$	TiO_2	Si
Bandgap (eV)	1.55	3.4	1.12
Relative dielectric constant	6.5	30	11.7
Affinity (eV)	3.9	4.0	4.05
Doping concentration (cm^{-3})(n type)	1×10^{17}	3×10^{19}	1×10^{15}
Electron/Hole mobility ($cm^2\ V^{-1}\ s^{-1}$)	$1\times10^{-3}/1\times10^{-3}$	$3\times10^{-6}/1\times10^{-6}$	1450/500
Electron/Hole lifetime (s)	$1\times10^{-6}/1\times10^{-6}$	$1\times10^{-9}/1\times10^{-9}$	$1\times10^{-4}/1\times10^{-4}$

Table S2. Dvice parameters of current typical perovskite-based PDs.

structure	active area (μm^2)	wavelength (nm)/ power (mW cm^{-2})	R (A W^{-1})	on/off ratio	D^* (Jones)	rise/decay time
$CH_3NH_3PbI_3$[4]	600×200	White/0.165	0.253[a)]	800[a)]	3.1×10^{12}[a)]	<40/50 ms
C8BTBT/$CH_3NH_3PbI_3$[5]	80×1000	532/0.37	14.7	1720	7.7×10^{12}	4.0/5.8 ms
$CH_3NH_3PbI_3$/graphene[6]	40×20000	532/0.014	2100	<2[a)]	~2×10^{11}	1.5/10 s
$CH_3NH_3PbI_3/WS_2$[7]	10×2000	505/0.5	2.1[a)]	5000[a)]	2×10^{12}	~3 s[a)]
$CH_3NH_3PbI_3$/GO[8]	100×200	660/0.02361	19200	<5	2.71×10^{13}	~10 ms
$CH_3NH_3PbI_3/TiO_2$/Si	**60×2000**	**White/0.5**	**62.5**	**6000**	**4.85×10^{13}**	**0.89/0.42 s**

[a)]these values were calculated based on the information provided in the papers.

Reference

[1] K. C. Kwon, K. Hong, Q. V. Le, S.Y. Lee, J. Choi, K.-B. Kim, S. Y. Kim, H. W. Jang, *Adv. Funct. Mater*. **2016**, *26*, 4213.

[2] X. Yi, Z. Huang, G. Lin, C. Li , S. Chen, W. Huang, J. Li, J. Wang, *Journal of Semiconductors* **2017**, *38*, 042001.

[3] S. Ke, S. Lin, X. Li, J. Li, J. Xu, C. Li, S. Chen, *Optics Express* **2016**, *24*, 1943.

[4] Y. Zhang, J. Du, X. Wu, G. Zhang, Y. Chu, D. Liu, Y. Zhao, Z. Liang, J. Huang, *ACS Appl.*

Mater. Interfaces **2015**, *7*, 21634.

[5] Y. Wang, Y. Zhang, Y. Lu, W. Xu, H. Mu, C. Chen, H. Qiao, *Adv. Opt. Mater.* **2015**, *3*, 1389.

[6] Z. Sun, L. Aigouy, Z. Chen, *Nanoscale* **2016**, *8*, 7377.

[7] C. Ma, Y. Shi, W. Hu, M.-H. Chiu, Z. Liu, A. Bera, F. Li, H. Wang, L.-J. Li, T. Wu, *Adv. Mater.* **2016**, *28*, 3683.

[8] L. Qian, Y. Sun, M. Wu, D. Xie, L. Ding, G Shi, *Adv. Mater*. **2017**, *29*, 1606175.